Comparison of near-threshold reactivity of ground-state and spin-orbit excited chlorine atoms with methane

Zee Hwan Kim, Andrew J. Alexander,[a] Hans A. Bechtel, and Richard N. Zare[b]
Department of Chemistry, Stanford University, Stanford, California 94305-5080

(Received 28 February 2001; accepted 18 April 2001)

A 4:1 mixture of CH_4 and BrCl diluted in He are coexpanded into a vacuum chamber and the reaction of methane with atomic chlorine is initiated by photolysis of BrCl. Near 420 nm, the resulting mixture of ground- and excited-state chlorine atoms have spatial anisotropies of $\beta_{\mathrm{phot}} = -0.7$ for the $Cl(^2P_{3/2})+Br$ channel and $\beta_{\mathrm{phot}} = +1.8$ for the $Cl^*(^2P_{1/2})+Br$ channel. The speed-dependent spatial anisotropy $\beta_{rxn}(v)$ of the $CH_3(v=0)$ reaction product is detected by 2 +1 resonance-enhanced multiphoton ionization. Our results indicate that the Cl^*+CH_4 reaction is unimportant in the near-threshold collision energy range of 0.13–0.16 eV, whereas the reaction with ground-state Cl atoms with CH_4 excited with one quantum in the ν_2 (torsion) or ν_4 (bending) mode is dominant. © *2001 American Institute of Physics.* [DOI: 10.1063/1.1378042]

I. INTRODUCTION

The reaction $Cl+CH_4 \rightarrow HCl+CH_3$ has drawn much attention from the environmental, experimental, and theoretical points of view. In addition to being an important reaction in combustion at high temperatures, this reaction is believed to be one of the termination steps of the ozone destruction cycle in the stratosphere. The modeling of these processes requires accurate parametrization of rate constants at wide temperature ranges, and has prompted detailed kinetics studies.[1–5] This reaction shows pronounced non-Arrhenius behavior at both low and high temperatures. Among other possible sources for this behavior, Ravishankara and Wine[3] postulated that the reactivity of spin-orbit excited $Cl^*(^2P_{1/2})$ is enhanced over that of ground-state $Cl(^2P_{3/2})$ and that this enhancement is mostly responsible for the non-Arrhenius behavior below 240 K. This postulate is based on the assumption that the extra spin-orbit energy (881 cm^{-1}) of Cl* is available for overcoming the reaction barrier, causing Cl* to be more reactive than Cl.

Often, Cl* reactivity has been believed to be the cause of disparities between the early kinetics data, but the proposed reaction, $Cl^*(^2P_{1/2})+CH_4 \rightarrow HCl(X\,^1\Sigma^+)+CH_3(\tilde{X}\,^2A_2'')$, is symmetry forbidden. It becomes possible only via a nonadiabatic transition between two different potential energy surfaces. Recent studies[1,4] show that the cross section for the Cl* quenching by CH_4 ($Cl^*+CH_4 \rightarrow Cl+CH_4$) is larger by more than 2 orders of magnitude than the reaction cross section for the ground-state reaction $Cl+CH_4 \rightarrow HCl+CH_3$. Therefore, for conventional kinetics experiments conducted under multiple-collision conditions, it can be argued that the role of Cl* reactivity is difficult to assess unless the Cl* reaction cross section is large enough to compete with the facile Cl* quenching channel. Matsumi *et al.*[1] attempted to measure the Cl^*+CH_4 reaction rate indirectly, and they have given an upper bound of 30% of total Cl* removal (Cl* reaction+quenching) rate. Nevertheless, the relative reactivity of Cl^*+CH_4 compared with $Cl+CH_4$ reactivity has not yet been measured.

A few experiments concerning the reactivity of spin-orbit excited halogen atoms (X^*) have been reported for the related reactions $X^*+H_2 \rightarrow HX+H$,[6–8] where $X=F$, Cl, and Br. Lee and Liu[6] observed that different methods for generating Cl atoms (photolysis of Cl_2 vs discharge of Cl_2) led to slightly different differential cross sections in their study of the $Cl+H_2 \rightarrow HCl+H$ reaction. They attributed the difference to the enhanced reactivity of Cl* over Cl. Nizkorodov *et al.*[8] studied the HF product state distribution of $F+H_2 \rightarrow HF+H$ at various collision energies. They noticed that part of the product distribution could not be explained by $F(^2P_{3/2})$ reacting with $H_2(v=0)$, but could be rationalized by assuming the reaction with $F^*(^2P_{1/2})$ occurs. Rigorous theoretical calculation of the effect of nonadiabatic interaction in a bimolecular reaction remains a challenging problem, even for simple chemical systems.[9]

In this paper, we report the first comparison of Cl and Cl* reactivity with CH_4 near the reaction threshold. We use what is called the photoloc (photo-initiated bimolecular reaction by law-of-cosines) technique.[10] The spatial anisotropy of the CH_3 product is measured and compared with the expected anisotropy for Cl* and Cl reacting with methane, thereby allowing us to directly assess the relative reactivity.

Figure 1 shows the energetics involved in $Cl/Cl^*+CH_4 \rightarrow HCl+CH_3$ reaction together with the total (translational+internal) energies involved in this work. The Cl atom reaction is endothermic by 600 cm^{-1},[11] whereas Cl* reaction is exothermic by 281 cm^{-1}, owing to the 881 cm^{-1} difference of the spin-orbit energy of Cl* compared to Cl. The activation barrier for the Cl–atom reaction, as derived from the Arrhenius fit of reaction rate at temperatures between 200 and 300 K, is 862 cm^{-1},[11] and the most recent

[a]Present address: Department of Chemistry, University of Edinburgh, West Mains Road, Edinburgh EH9 3JJ, United Kingdom.
[b]Author to whom correspondence should be addressed. Electronic mail: zare@stanford.edu

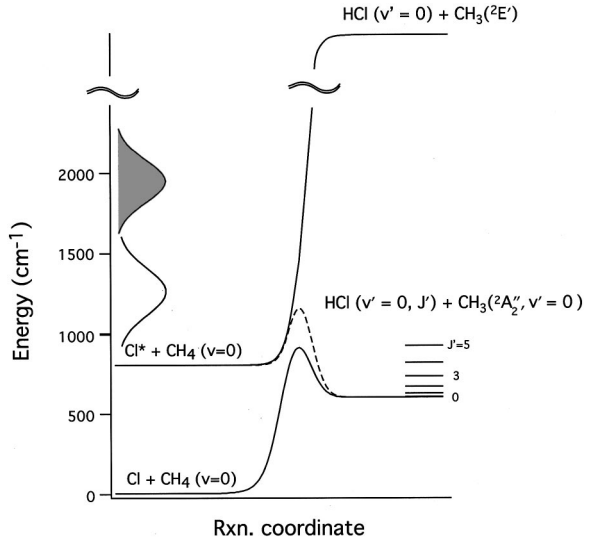

FIG. 1. Energetics of the reaction of Cl/Cl* with CH_4. $Cl(^2P_{3/2})+CH_4$ correlates adiabatically to $HCl+CH_3(^2A_2'')$ (solid line). $Cl^*(^2P_{1/2})+CH_4$ correlates to $HCl+CH_3(^2E')$ that is energetically inaccessible with the collision energies used (solid line). The reaction $Cl^*(^2P_{1/2})+CH_4 \rightarrow HCl+CH_3(^2A_2'')$ requires nonadiabatic transition between the potential energy surfaces (shown in dashed line, effective reaction barrier height is arbitrarily drawn). The *total* energies are measured from the bottom of $Cl+CH_4(\nu=0)$, and their spread for $Cl+CH_4$ (solid curve) and Cl^*+CH_4 (shaded curve) at $E_{coll}=0.14$ eV are represented by the Gaussian distributions that would result from a estimated beam translational temperature of 15 K (see Ref. 29). Note that although the center-of-mass translational energy of $Cl+CH_4$ is slightly larger than that of Cl^*+CH_4 for a given wavelength of photolysis, the *total* energy available for the reaction is higher for the Cl^*+CH_4.

semiempirical potential energy surface by Corchado *et al.*[12] predicts a barrier height of 1574 cm^{-1}, including the zero-point energies of reagents and products. It should be noted that the experimental activation barrier from the low-temperature rate measurement underestimates the actual barrier height because of the non-Arrhenius behavior at low temperature. As such, the theoretical reaction barrier is usually larger than the activation energy. The calculations[12–15] indicate: (1) the transition state is collinear along the Cl–H–C axis; (2) the reaction has a ''late'' barrier located in the exit valley; and (3) the reaction rate is enhanced by C–H stretching mode excitation of CH_4. The series of experiments by Zare and co-workers[10,16–18] agree with these results.

We employed photodissociation of BrCl near 420 nm as a source of Cl and Cl* atoms. Photodissociation of BrCl at this wavelength involves two major pathways: the Cl+Br channel via $C\,^1\Pi(1)-X\,^1\Sigma(0^+)$, and the Cl*+Br channel mostly via $B\,^3\Pi(0^+)-X\,^1\Sigma(0^+)$ transitions. The relative cross section of Cl*+Br vs Cl+Br and the spatial anisotropies at various photolysis wavelengths have been characterized by Cao *et al.*[19] and by Cooper *et al.*[20] The yield of Cl* changes from 37% to 57% as the photodissociation wavelength varies from 410 to 430 nm. The spatial anisotropy of each channel has a different value and changes slightly across the wavelengths used. Although the center-of-mass *translational* energy (E_{coll}) is slightly smaller for the Cl* reaction based on energy conservation, the *total* energy available for the reaction is larger for the Cl* reaction for a given photolysis wavelength of the BrCl molecule (see Fig. 1).

The spatial anisotropy of the reaction product $\beta_{rxn}(\nu)$ from a bimolecular reaction initiated by a photolysis process that is characterized by a spatial anisotropy β_{phot} is determined by

$$\beta_{rxn}(\nu)=\beta_{\text{phot}}P_2(\cos\alpha), \tag{1}$$

where P_2 is the second-order Legendre polynomial and α is the angle between the center-of-mass velocity and the product velocity vectors, as determined by the kinematics of the reaction. From Eq. (1), it is clear that the laboratory velocity resolved (hence angle α resolved) spatial anisotropy of the particular product is directly proportional to the spatial anisotropy of the photolysis step. The prediction of spatial anisotropy however does not require knowledge of the differential cross section of the product. In this experiment, we have two dissociation channels (Cl+Br and Cl*+Br) for the photolysis step. The measured spatial anisotropy of the CH_3 product is an average of two spatial anisotropies of the CH_3 product that are associated with each channel in the photolysis step, being weighed by the *relative reactivity of* Cl vs Cl* and by the relative flux of Cl vs Cl*. Therefore, with a knowledge of the relative yield for Cl and Cl* and the spatial anisotropies for Cl and Cl* from the photolysis, it is possible to obtain the relative reactivity of Cl and Cl* with methane by measuring the CH_3 product spatial anisotropy.

II. EXPERIMENT

Details of the experimental setup and techniques have been discussed previously.[10,21] BrCl was synthesized in a glass bulb by mixing Cl_2 and Br_2 with 1:3 ratio, and waiting for >30 min. Br_2 (Aldrich, 99.5+% stated purity) is degassed by several freeze–pump–thaw cycles with liquid nitrogen and dry ice before mixing with Cl_2 (Matheson, 99.999%). Because the equilibrium constant for $Br_2+Cl_2 \leftrightarrow 2BrCl$ is only 7 at room temperature,[20] separation of BrCl from unreacted Br_2 and Cl_2 is not feasible. Unreacted Cl_2 and Br_2 can be photolyzed by 420 nm to produce Cl, Cl*, Br, and Br* atoms. However, the photodissociation cross section of Cl_2 at this wavelength is minimal compared with the cross section of BrCl, and the kinetic energy of Cl atoms produced from Cl_2 at this wavelength is too low to overcome the endothermicity (660 cm^{-1}) to generate product. Also, we confirmed experimentally that neither the presence of Br_2 nor Cl_2 produced reaction signal, by running control experiments with mixes of $Br_2/CH_4/He$ and $Cl_2/CH_4/He$. The BrCl was further mixed with CH_4 (Matheson, 99%) and He (Liquid Carbonic, 99.995%) with a ratio of $BrCl:CH_4:He=1:4:5$ and delivered to the pulsed nozzle (General valve series-9, 0.6 mm orifice size) where it was supersonically expanded into the ionization region of a core-extracted Wiley–McLaren type time-of-flight (TOF) spectrometer. The reaction was initiated by a photolysis beam (410–430 nm) that was produced by frequency doubling (by a BBO crystal) the Nd:YAG laser pumped dye laser output (PL9020 and ND6000, Continuum; LDS867, Exciton). The CH_3 products were allowed to accumulate for

TABLE I. Spatial anisotropies of BrCl photolysis and the relative yields of Cl*.

λ_{phot} (nm)	E_{coll} (eV)	%Cl*[a]	β_{phot} (Cl)	β_{phot} (Cl*)
410	0.13	37	-0.76 ± 0.02[c]	1.88 ± 0.02[c]
420	0.14	50[b]	-0.69 ± 0.01	$1.79\pm.04$
430	0.16	57	-0.47 ± 0.02	1.82 ± 0.04

[a]See Cao *et al.*[19] See also Cooper *et al.*[20]
[b]Value at 421.7nm.
[c]Uncertainties shown are 1 σ.

60–100 ns before being ionized by $2+1$ resonantly enhanced multiphoton ionization (REMPI) through the $3p_z\ ^2A_2''-\tilde{X}\ ^2A_2''$ transition.[22] Frequency-doubled light near 333.3 nm from a Nd:YAG pumped dye laser system (DCR-2A, Spectra-Physics; FL2002, Lambda Physik; DCM and LDS698, Exciton) drove the REMPI process. The resulting ions were detected with microchannel plates. The reaction products were distinguished from background signals through time–jump subtraction.[21] A photoelastic modulator (PEM-80, Hinds International Inc.) flipped the direction of the linear polarization of the photolysis laser beam between parallel and perpendicular to the TOF axis on an every-other-shot basis. The intensity difference of the parallel and the perpendicularly polarized photolysis beam was measured to be less than 0.2%. The TOF profiles taken with parallel photolysis polarization ($\mathbf{I}_{\parallel}$) and perpendicular polarization ($\mathbf{I}_{\perp}$) were separately averaged. The isotropic ($\mathbf{I}_{ISO}=\mathbf{I}_{\parallel}+2\mathbf{I}_{\perp}$) and anisotropic ($\mathbf{I}_{ANISO}=2(\mathbf{I}_{\parallel}-\mathbf{I}_{\perp})$) components of the TOF profiles were used to extract the speed dependent spatial anisotropy of the CH_3 products by fitting these components of the TOF profiles to basis functions generated by Monte Carlo simulations.[10]

Spatial anisotropies of BrCl(β_{phot}) at the wavelengths 410, 420, and 430 nm that are needed for the analysis and the interpretation of data were obtained by a separate experiment. The Cl($^2P_{3/2}$) and Cl*($^2P_{1/2}$) photofragments were ionized via $2+1$ REMPI within 10 ns of the photolysis pulse, and the isotropic and anisotropic components of TOF profiles were analyzed to obtain the β_{phot} parameters.

III. RESULTS AND DISCUSSION

A. Spatial anisotropy of BrCl

Table I lists the measured spatial anisotropies (β_{phot}) at the wavelengths 410, 420, and 430 nm. The Cl* channel shows strong parallel character ($\beta\sim+2$), whereas Cl channel shows perpendicular character ($\beta\sim-1$), which slightly changes across the wavelengths used. To check for possible orbital alignment[23] of the Cl photofragments (Cl* atoms cannot show alignment) that may affect our spatial anisotropy measurement, we varied the direction of polarization of probe beam, and obtained the same values within the error bars. Therefore, the measured spatial anisotropies do not suffer from the interference caused by the orbital alignment of chlorine atoms. The contribution from ''hot-band'' dissociation from BrCl($\nu''=1$ or 2)$\rightarrow$Br+Cl/Cl*[24] is found to be negligible at these wavelengths based on our analysis of TOF profiles. Our results show reasonable agreement with the results of Cooper *et al.*,[20] although slight systematic differences exist, especially for the Br+Cl* channel.

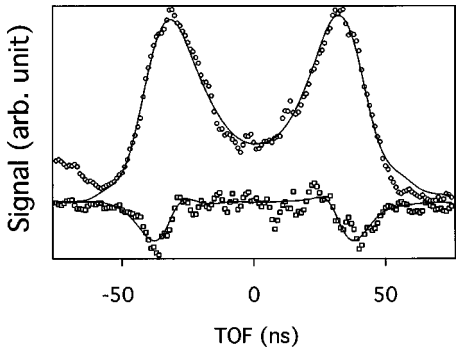

FIG. 2. Isotropic (open circles $\mathbf{I}_{ISO}$) and anisotropic (open squares $\mathbf{I}_{ANISO}$) components of time-of-flight (TOF) profile of CH_3 product at 0.14 eV collision energy. Also shown are the results of the fitting to the basis functions (solid curves). The small bump near -75 ns is an artifact produced perhaps by nonresonant dissociative multiphoton ionization of CH_4 or pump oil by the 420 nm photolysis beam, and it does not interfere with our analysis.

B. Speed distribution and spatial anisotropy of the CH_3 product

Figure 2 shows the isotropic and anisotropic components of representative $CH_3(\nu=0)$ TOF profiles (via the Q branch of the band) at the collision energy $E_{coll}=0.14$ eV ($\lambda_{phot}=420$ nm), along with the fit to the basis functions. Overall shapes of the TOF profiles are very similar to the profiles obtained by Kandel and Zare[21] with pure Cl($^2P_{3/2}$) ground-state reaction at a similar collision energy. We were not able to detect $CH_3(v_2=1)$ product via the 2_1^1 band within our signal-to-noise ratio, which gives an upper bound for the production of $CH_3(v_2=1)$ of $\leqslant$1% relative to $CH_3(\nu=0)$. The results of the fit give the laboratory speed distribution and the speed-dependent spatial anisotropy $\beta_{rxn}(\nu)$ of $CH_3(\nu=0)$ product, which are shown in Fig. 3.

The physically allowed speed of the CH_3 product is determined by the kinematics of the reaction, and the shape of the distribution within the allowed speed range is dependent on the differential cross section of the reaction product. As seen in Fig. 3(A), a significant portion of the distribution lies outside of the speed range that is allowed for $Cl+CH_4(\nu=0)$ reaction at $E_{coll}=0.14$ eV, which indicates that one or more other reaction channels contribute. Figure 3(B) shows the spatial anisotropy of the reaction product, $\beta_{rxn}(\nu)$ for the CH_3 at $E_{coll}=0.14$ eV, where the Cl* yield is 50%. The measured spatial anisotropy is plotted along with four calculated curves. These show the predicted $\beta_{rxn}(\nu)$ values for the $Cl+CH_4(\nu=0)$ [curve (A), thin solid line], $Cl+CH_4[\nu_4(\text{bending})=1]$ [curve (B), thick solid line], $Cl+CH_4[\nu_2(\text{torsion})=1]$ [curve (C), dashed-dotted line], and $Cl^*+CH_4(\nu=0)$ [curve (D), dotted line]. The spatial anisotropy could be extracted reliably within the speed range that covers 99.5% of the $CH_3(\nu=0)$ speed distribution. Therefore, the trends in measured spatial anisotropy reflect the behavior of almost all of the CH_3 products. The measured spatial anisotropy does not have any similarity to the curve (D) nor can any combination of curves that include curve (D)

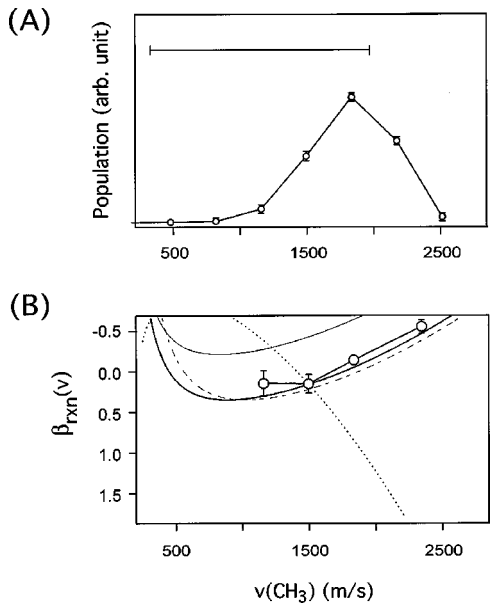

FIG. 3. (A) Speed distribution of CH_3 product (open circles). The scale bar on the top shows the laboratory frame speed range allowed for $Cl+CH_4(\nu=0)\rightarrow HCl+CH_3$. (B) Speed-dependent spatial anisotropy $\beta_{rxn}(v)$ for CH_3 product 0.14 eV collision energy (open circles). The experimental data are presented along with four curves showing the predicted spatial anisotropy for the $Cl+CH_4(\nu=0)$ (thin solid line), $Cl+CH_4(\nu_4=1)$ (thick solid line), $Cl+CH_4(\nu_2=1)$ (dashed-dotted line), and $Cl^*+CH_4(\nu=0)$ (dotted line). The data indicate that reaction with ν_2 or $\nu_4=1$ excited methane is dominant. Error bars represent 2 σ of multiple (at least five) sets of measurements. The range of the y axis is chosen such that the minimum value corresponds to $\beta_{\text{phot}}(\text{Cl})$, and the maximum value to $\beta_{\text{phot}}(\text{Cl}^*)$.

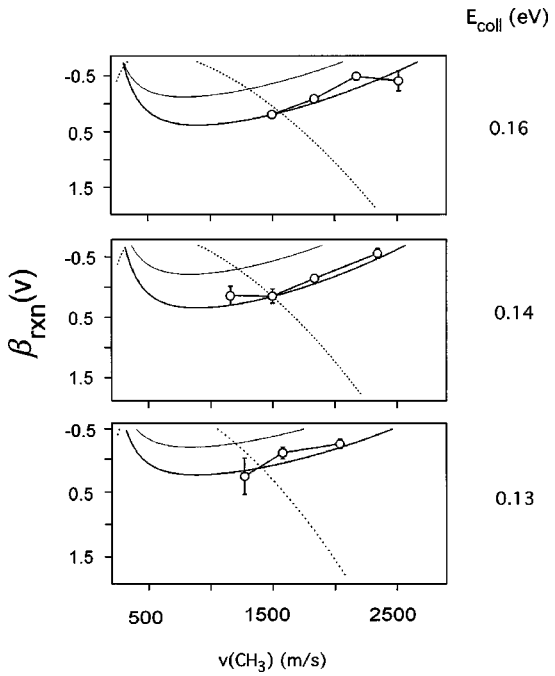

FIG. 4. Spatial anisotropies (open circles) for CH_3 products at collision energies $E_{\text{coll}}=0.16$ (top), 0.14 (middle), and 0.13 (bottom) eV. Also shown are $Cl+CH_4(\nu=0)$ (thin solid line), $Cl+CH_4(\nu_4=1)$ (thick solid line), and $Cl^*+CH_4(\nu=0)$ (dotted line).

provide a reasonable fit to the measured anisotropy. Instead, curves (B) and (C), corresponding to the reaction with $\nu_4=1$ and $\nu_2=1$ vibrationally excited methane, respectively, provide an exceedingly good match to the data, with curve (B) giving a marginally better agreement than curve (C) to the measured anisotropy. This result indicates that the previously proposed Cl* reactivity with $CH_4(\nu=0)$ is unimportant compared with ground-state Cl reactivity with $CH_4(\nu_2 \text{ or } \nu_4=1)$. The latter accounts for only ~1% of the CH_4 population in our beam expansion. Similar behavior, the enhanced reactivity of $Cl(^2P_{3/2})+CH_4(\nu_2 \text{ or } \nu_4=1)$ over $Cl(^2P_{3/2})+CH_4(\nu=0)$ was first observed by Kandel and Zare.[21]

Although the Cl* reaction channel is exothermic, it is possible that the reaction barrier might be higher than that of the Cl–atom reaction owing to nonadiabatic interaction near the barrier. Clearly, the barrier height for the Cl* reaction is not smaller than that of the Cl–atom reaction as measured from the energy level of $Cl(^2P_{3/2})+CH_4$. Therefore, it is possible that the collision energy of 0.14 eV might not be sufficient to surmount the Cl* reaction barrier. On the other hand, Cl* reactivity would be most noticeable at lower collision energies, where the total energies are closer or below reaction threshold for $Cl+CH_4(\nu=0)$. To check for these possibilities, we tuned the 0.14 eV collision energy to higher and lower values. Experimentally, tuning of the collision energy is limited by two factors. The Cl* branching ratio of BrCl photolysis drops sharply at photolysis wavelengths below 410 nm.[19] At photolysis wavelengths longer than 430 nm, the CH_3 signal level drops significantly such that it does not allow us to obtain a reliable spatial anisotropy of the product. In Fig. 4, we compare the results of the analysis at $E_{\text{coll}}=0.13$, 0.14, and 0.16 eV, with the calculated anisotropies as described in the previous paragraph. At $E_{\text{coll}}=0.13\,\text{eV}$ ($\lambda_{\text{phot}}=430\,\text{nm}$), an appreciable portion of the $Cl+CH_4(\nu=0)$ collision energy distribution has lower energy than the activation energy of 960 cm^{-1} (see Fig. 1). Again, all of the measured spatial anisotropies lie close to the curves expected for $Cl+CH_4(\nu_2 \text{ or } \nu_4=1)\rightarrow HCl+CH_3$. Therefore, we conclude that the Cl^*+CH_4 reaction is not important in the collision energy range between 0.13 and 0.16 eV; instead, we suggest the dominant role of reaction of methane molecules excited with one quantum of vibration in ν_2 or ν_4 with ground-state Cl atoms. Although we cannot claim that the $Cl^*+CH_4(\nu=0)$ channel is less reactive than $Cl+CH_4(\nu=0)$, we can safely state that the $Cl^*+CH_4(\nu=0)$ reaction is less reactive than the $Cl+CH_4(\nu_2 \text{ or } \nu_4=1)$ reaction. Moreover, we can set a conservative upper bound for the Cl* reactivity to be $\leqslant 1\%$[25] of the reactivity of $Cl+CH_4(\nu_2 \text{ or } \nu_4=1)$ reaction near reaction threshold.

In 1972, Truhlar[26] and Muckerman and Newton[27] first discussed whether the mechanism for the $F^*+H_2\rightarrow HF+H$ reaction channel should be described as statistical vs adiabatic. In the statistical limit, each spin-orbit state contributes according to its multiplicity to the overall cumulative probability, thus predicting appreciable contributions from the spin-orbit excited halogen atom. In the adiabatic limit, no F* reactivity is predicted to generate $HF(^1\Sigma^+)+H$ products. Schatz,[28] in his theoretical work on $Cl(^2P_J)+HCl\rightarrow HCl+Cl(^2P_{J'})$ (where $J,J'=1/2$ or 3/2) reaction, generalized statistical and adiabatic approaches. Although

the calculated overall rate constant is shown to be rather insensitive to the degree of nonadiabatic interaction for this particular reaction, Schatz claimed that this system follows the adiabatic limit for a physically appropriate value of spin-orbit coupling for the Cl atom. In sharp contrast, several rate constant calculations on the $Cl+CH_4$ reaction[12,15] have been based on a statistical treatment of the Cl* reaction channel, including significant contributions from the Cl^*+CH_4 reaction.

Kandel and Zare[21] estimated the low-frequency torsion (ν_2) or bending mode (ν_4) enhancement to be 200 times compared to the $Cl+CH_4(\nu=0)$ reaction, which is larger than the enhancement factor of 30 for the asymmetric stretching mode excited $(\nu_3=1)CH_4$ reaction.[17] At this point, it is not clear why the bending mode or the torsion mode excitation shows more enhancement than the asymmetric stretching mode, recalling that all theoretical calculations[12–15] support a collinear Cl–H–C transition-state geometry. Kandel and Zare also suggested that the bending or torsion mode enhancement might contribute to the non-Arrhenius behavior at low temperatures. Theoretical studies by Duncan and Truong[15] and Corchado *et al.*[12] predict modest to large enhancement of reactivity by bending mode excitation caused by the lowering or removal of the barrier to reaction. Their calculations, at the same time, suggest that the major contribution to the non-Arrhenius behavior is quantum mechanical tunneling rather than bending mode enhancement. Recent work by Michelsen and Simpson[2] suggest a modest contribution of bending enhancement to the non-Arrhenius behavior, with the major contribution from tunneling.

Our results set a new upper bound for Cl* reactivity with CH_4, and they rule out the possibility of the role of Cl* reactivity in the explanation of the non-Arrhenius behavior at low temperatures. Also, we observed the dominant role of reaction of ground state chlorine atom with bending or torsion mode excited methane at near-threshold collision energies. Further detailed studies may reveal the nature of the bending and torsion mode enhancement in the $Cl+CH_4$ reaction.

ACKNOWLEDGMENTS

The authors thank Andrew J. Orr-Ewing, S. Alex Kandel, and Hope A. Michelsen for valuable discussions and Andrew J. Orr-Ewing for providing them with unpublished data on BrCl photofragment anisotropies. One of the authors (H.A.B.) also thanks the National Science Foundation for a graduate fellowship. This work was supported by the National Science Foundation under Grant No. NSF-CHE-99-00305.

[1] Y. Matsumi, K. Izumi, V. Skorohodov, M. Kawasaki, and N. Tanaka, J. Phys. Chem. A **101**, 1216 (1997).
[2] H. A. Michelsen and W. R. Simpson, J. Phys. Chem. A **105**, 1476 (2001).
[3] A. R. Ravishankara and P. H. Wine, J. Chem. Phys. **72**, 25 (1980).
[4] G. S. Tyndall, J. L. Orlando, and C. S. Kegley-Owen, J. Chem. Soc., Faraday Trans. **91**, 3055 (1995).
[5] J. S. Pilgrim, A. McIlroy, and C. A. Taatjes, J. Phys. Chem. A **101**, 1873 (1997).
[6] S.-H. Lee and K. Liu, J. Chem. Phys. **111**, 6253 (1999).
[7] D. J. Nesbitt and S. R. Leone, J. Chem. Phys. **73**, 6182 (1980).
[8] S. A. Nizkorodov, W. W. Harper, W. B. Chapman, B. W. Blackmon, and D. J. Nesbitt, J. Chem. Phys. **111**, 8404 (1999).
[9] D. E. Manolopoulos, J. Chem. Soc., Faraday Trans. **93**, 673 (1997).
[10] W. R. Simpson, T. P. Rakitzis, S. A. Kandel, A. J. Orr-Ewing, and R. N. Zare, J. Chem. Phys. **103**, 7313 (1995).
[11] R. Atkinson, D. L. Baulch, R. A. Cox, J. R. F. Hampson, J. A. Kerr, M. J. Rossi, and J. A. Troe, J. Phys. Chem. Ref. Data **28**, 191 (1999).
[12] J. C. Corchado, D. G. Truhlar, and J. Espinosa-García, J. Chem. Phys. **112**, 9375 (2000).
[13] A. Gonzalez-Lafont, T. N. Truong, and D. G. Truhlar, J. Chem. Phys. **95**, 8875 (1991).
[14] K. D. Dobbs and D. A. Dixon, J. Phys. Chem. **98**, 12584 (1995).
[15] W. T. Duncan and T. N. Truong, J. Chem. Phys. **103**, 9642 (1995).
[16] T. P. Rakitzis, S. A. Kandel, and R. N. Zare, J. Chem. Phys. **107**, 9382 (1997).
[17] W. R. Simpson, T. P. Rakitzis, S. A. Kandel, T. Lev-On, and R. N. Zare, J. Phys. Chem. **100**, 7933 (1996).
[18] A. J. Orr-Ewing, W. R. Simpson, T. P. Rakitzis, S. A. Kandel, and R. N. Zare, J. Chem. Phys. **106**, 5961 (1997).
[19] J. Cao, H. P. Look, and C. X. W. Qian, Can. J. Chem. **72**, 758 (1994).
[20] M. J. Cooper, P. J. Jackson, L. J. Rogers, A. J. Orr-Ewing, and B. J. Whitaker, J. Chem. Phys. **109**, 4367 (1998).
[21] S. A. Kandel and R. N. Zare, J. Chem. Phys. **109**, 9719 (1998).
[22] J. W. Hudgens, T. G. DiGiuseppe, and M. C. Lin, J. Chem. Phys. **79**, 571 (1983).
[23] T. P. Rakitzis, S. A. Kandel, A. J. Alexander, Z. H. Kim, and R. N. Zare, J. Chem. Phys. **110**, 3351 (1999).
[24] A. J. Orr-Ewing (private communications, 2001): The β parameters at longer wavelengths 460–560 nm depend very strongly on the vibrational quantum number of the BrCl parent. This ''hot-band'' ($\nu''=1$ or 2) photodissociation is observed to give different β parameters from those of $BrCl(\nu''=0)$ photolysis. This is also observed for IBr and it is a consequence of Franck–Condon factors for excitation to different repulsive surfaces. See also E. Wrede, S. Laubach, S. Schulenburg, A. Brown, E. R. Wouters, A. J. Orr-Ewing, and M. N. R. Ashfold, J. Chem. Phys. **114**, 2629 (2001).
[25] If we assume that CH_3 product distributions from Cl and Cl* reactions give the same shape of speed distribution, the effective spatial anisotropy $\beta_{\text{eff}}(v)$ is given by the reactivity and flux weighted average of two reactions: $\beta_{\text{eff}}(v)=(1-f)\beta(v)+f\beta^*(v)$, where $\beta(v)$, and $\beta^*(v)$ are the calculated spatial anisotropies for $Cl+CH_4$ (ν_4 or $\nu_2=1$) and $Cl^*+CH_4(\nu=0)$ reactions, and $f=wu^*[Cl^*][CH_4(\nu=0)]/(wu^*[Cl^*][CH_4(\nu=0)]+u[Cl][CH_4(\nu_4 \text{ or } \nu_2=1)])$ (0.99 for $E_{\text{coll}}=0.14$ eV). The w is the relative reaction cross section of Cl* atoms, and u and u^* are center of mass speeds associated with Cl and Cl*, respectively. The w is increased from zero until the $\beta_{\text{eff}}(v)$ curve lies completely outside of the 1 σ of the measured spatial anisotropy for all speeds. We chose w as the upper bound for the Cl* reactivity.
[26] D. G. Truhlar, J. Chem. Phys. **56**, 3189 (1972).
[27] J. T. Muckerman and M. D. Newton, J. Chem. Phys. **56**, 3191 (1972).
[28] G. C. Schatz, J. Phys. Chem. **99**, 7522 (1995).
[29] W. J. van der Zande, R. Zhang, and R. N. Zare, J. Chem. Phys. **95**, 8205 (1991).